*Clays and Clay Minerals*, Vol. 43, No. 1, 39–50, 1995.

# DISSOLUTION PROCESS OF PHLOGOPITE IN ACID SOLUTIONS

YOSHIHIRO KUWAHARA AND YOSHIKAZU AOKI

Department of Earth and Planetary Sciences, Faculty of Science
Kyushu University, Fukuoka 812, Japan

**Abstract**—The alteration experiments of phlogopite with 0.01 N HCl solution containing 0.1 M NaCl at 50°, 80° and 120°C have been carried out to aid in the understanding of the dissolution process of mica and the formation of secondary phases such as vermiculite and interstratified mica/vermiculite. Twenty milligrams of phlogopite samples were suspended in 20 ml or 100 ml of leaching solution.

In these experiments, the dissolution of phlogopite occurred incongruently, where the preferential release of K occurred in almost all stages of the alteration reaction. In the 100 ml experiments, the priority in dissolution in the initial stage was in the order; K > Fe > Mg, Al > Si. This supports that phlogopite leaching is controlled by the mineral structure. At 80° and 50°C in the 20 ml experiments, the release of all elements except for K was nearly congruent. At 120°C in the 20 ml experiments, the dissolution was outwardly incongruent, which Fe decreased remarkably after six days and Al was released most slowly compared with all other elements in phlogopite. This is probably due to the precipitation of secondary phases such as aluminum and iron oxides and/or hydroxides.

Vermiculite and R1-type interstratified mica/vermiculite, containing 70 ~ 50% mica, were formed in the alteration process of phlogopite. The following two processes were confirmed for the formation of interstratified structure: Interstratified structure was formed (1) directly from phlogopite or (2) from vermiculite which was produced earlier from phlogopite by regaining of K from the ambient solution. It may depend on the release rate of K from phlogopite whether mica-vermiculite layer sequences develop or vermiculite-vermiculite sequences do.

**Key Words**—Alteration, Biotite, Dissolution, Interstratification, Leached layer, Mica/vermiculite, Phlogopite, Transmission electron microscopy, Vermiculite.

## INTRODUCTION

Alteration of micas has been experimentally carried out by several investigators to simulate natural weathering and the hydrothermal alteration processes. Barshad (1948) found that K in biotite was replaced with hydrated Mg when in contact with a $MgCl_2$ solution. Since then, the exchange reaction experiments of interlayer K in mica with salt solutions have been actively studied (Norrish 1973), and the diffusion control model has been proposed to explain the K exchange mechanism (Mortland 1958, Reed and Scott 1962, Leonard and Weed 1970).

Schnitzer and Kodama (1976) pursued compositional changes in a fulvic acid solution on dissolution of three micas (phlogopite, biotite, and muscovite) and showed congruent dissolution. However, phlogopite dissolved incongruently when in contact with Ca-bearing hydrochloric acid solution produces vermiculite and interstratified mica/vermiculite (Inoue *et al* 1981).

Biotite and phlogopite can transform to vermiculite, directly (Walker 1949, Wilson 1966) or through an interstratified structure (Boettcher 1966, Wilson 1970, Brindley *et al* 1983) during natural weathering or hydrothermal alteration. Transmission electron microscopic (TEM) study for the different stages of mica alteration have been carried out by Banfield and Eggleton (1988) and Reichenbach *et al.* (1988) to demonstrate the structural modification. Rhcades and Coleman (1967) and Sawhney (1969) represented that the reverse transformation of vermiculite to mica also takes place through an interstratified structure. Tsuzuki (1985) has commented that alteration products such as vermiculite and interstratified mica/vermiculite may be a leached layer which is formed throughout a mica crystal. The investigation on the formation of the leached layer constitutes an important contribution to the understanding of alteration of micas, but more information is necessary.

Phlogopite was reacted with Na-bearing hydrochloric acid solutions to better understand the dissolution process of micas and the formation of secondary phases. Both solution and solid data were monitored as a function of time at 50°, 80°, and 120°C.

## EXPERIMENTAL

### *Material*

Phlogopite from the Pote Mine, North Korea was used throughout this study. It is of 1 M polytype with $a_0$ = 5.31 Å, $b_0$ = 9.20 Å, $c_0$ = 10.22 Å, $\beta$ = 100.12° and has the chemical composition shown in Table 1.

The large flakes were dry-ground in a ball mill, the sample was size fractionated by sedimentation and the 5–20 $\mu$m fraction was used in these experiments.

### *Experimental procedure*

Hydrothermal runs were performed in sealed Teflon vessels placed in a thermostated dry oven. Temperatures were maintained at 50°, 80°, and 120°C, and were

Copyright © 1995, The Clay Minerals Society



https://doi.org/10.1346/CCMN.1995.0430105 Published online by Cambridge University Press

Table 1. Chemical composition of phlogopite used as the starting material by EPMA.

| | wt. % | Number of cations and F atoms on the basis of $O_{20}(OH)_4$ | |
|---|---|---|---|
| $SiO_2$ | 40.74 | Si | 5.74 |
| $Al_2O_3$ | 14.48 | Al | 2.26 |
| $TiO_2$ | 0.54 | Ti | |
| $Fe_2O_3$ | 0.47 | Σ tet | 8.00 |
| FeO | 1.44 | Al | 0.15 |
| MnO | 0.05 | Ti | 0.06 |
| MgO | 26.56 | $Fe^{3+}$ | 0.05 |
| CaO | 0.00 | $Fe^{2+}$ | 0.17 |
| BaO | 0.20 | Mn | 0.01 |
| $Na_2O$ | 0.36 | Mg | 5.58 |
| $K_2O$ | 10.03 | Σ oct | 6.02 |
| $H_2O^+$ | 3.84 | Ca | 0.00 |
| $H_2O^-$ | | Ba | 0.01 |
| F | 2.17 | Na | 0.10 |
| F=O | 0.91 | K | 1.80 |
| Cl | 0.04 | Σ interl | 1.91 |
| Cl=O | 0.01 | F | 0.97 |
| Total | 100.00 | Cl | 0.01 |

known with an accuracy of ±5°C but were fluctuating less than 1°C for each run. Twenty milligrams of phlogopite samples were suspended in 20 ml or 100 ml of leaching solution in order to examine the volume effect of the solution. Here, 0.01 N HCl solutions containing 0.1 M NaCl were used as the leaching solution. Run times ranged from one hour to 44 days. After the desired run time the suspensions were immediately centrifuged. The solid run products were washed with deionized water to remove soluble chlorides. Each reacted solution was transferred to a polyethylene bottle for solution analysis.

The solid run products were characterized by XRD. The XRD patterns of oriented aggregates on glass slide were recorded with a JEOL JDX-7S X-ray diffractometer, using Ni filtered Cu radiation. Glycerol solvation after Mg-saturation for alteration products were performed to characterize vermiculite. Relative amount of solid phases in each run product were determined by calibration curve obtained from integrated intensity ratio for component minerals. The integrated intensity and accurate peak positions for the coefficient of variation (CV) value of interstratified mica/vermiculite were estimated from the X-ray data using an NEC PC-9801 series personal computer and the profile fitting program made by Nakamuta *et al* (1991). The concentrations of Si, Al, Fe, Mg and K in solutions after reaction were measured using a Seiko SPS 1200AR ICP-AES. The pH of the reacted solution was measured with a Horiba pH meter D13.

TEM and analytical electron microscopic (AEM) study was made on samples both before and after dissolution to demonstrate the structural modification in the alteration process of mica. The specimen for TEM was prepared as follows: The samples were dispersed in water by five min of exposure to ultrasonic vibration, and a small drop of this suspension was dried on a copper grid covered with a microgrid. Selected samples were examined using a JEOL JEM-200CX TEM and JEM-2000FX AEM in the HVEM Laboratory of Kyushu University, operating at 200 kV.

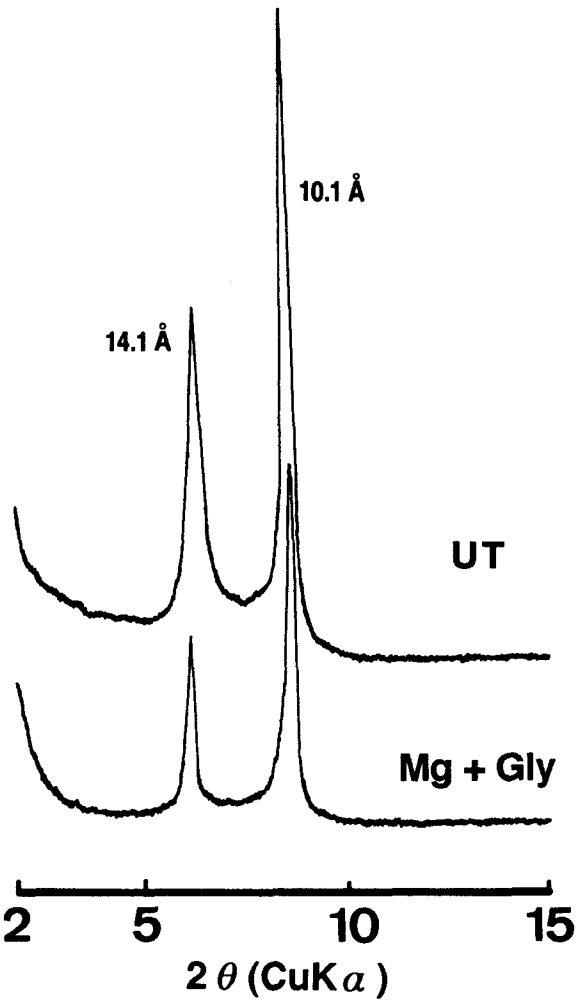



Figure 1. X-ray powder diffraction patterns of alteration product at two days of reaction at 50°C in the 100 ml experiments. UT: untreated. Mg+Gly: Glycerol solvation after Mg-saturation.

## RESULTS

### *Alteration products*

Vermiculite and interstratified mica/vermiculite were identified by XRD diagrams as the alteration products. Those formed in the present experiments did not expand with glycerol solvation after Mg-saturation (Figure 1). The mineral proportions in each run product are given in Table 2. Interstratified mica/vermiculite increased gradually with time both in the 20 ml and

https://doi.org/10.1346/CCMN.1995.0430105 Published online by Cambridge University Press

Table 2. Experimental results for 20 ml and 100 ml experiments.

| T (°C) | Volume of solution (ml) | Conc. of HCl (M) | Duration (days) | Solid phases present[1] (wt. %) P | V | P/V |
|---|---|---|---|---|---|---|
| 120 | 20 | 0.01 | 1 hour | 98 | 2 | — |
| | | | 2 h | 95 | 5 | — |
| | | | 4 h | 83 | 7 | 10 |
| | | | 8 h | 82 | — | 18 |
| | | | 12 h | 61 | — | 39 |
| | | | 1 | 69 | — | 31 |
| | | | 2 | 65 | — | 35 |
| | | | 4 | 54 | — | 46 |
| | | | 8 | 48 | — | 52 |
| | | | 12 | 40 | — | 60 |
| | | | 16 | 37 | — | 63 |
| | | | 20 | 25 | — | 75 |
| | | | 28 | — | — | 100 |
| | | | 36 | — | — | 100 |
| 80 | 20 | 0.01 | 1 | 85 | 4 | 11 |
| | | | 2 | 79 | — | 21 |
| | | | 4 | 75 | — | 25 |
| | | | 8 | 72 | — | 28 |
| | | | 12 | 70 | — | 30 |
| | | | 16 | 70 | — | 30 |
| | | | 20 | 67 | — | 33 |
| | | | 28 | 70 | — | 30 |
| | | | 36 | 69 | — | 31 |
| 50 | 20 | 0.01 | 1 | 98 | 2 | — |
| | | | 2 | 80 | 8 | 12 |
| | | | 4 | 87 | 2 | 11 |
| | | | 8 | 77 | — | 23 |
| | | | 12 | 83 | — | 17 |
| | | | 16 | 75 | — | 25 |
| | | | 20 | 78 | — | 22 |
| | | | 28 | 77 | — | 23 |
| | | | 36 | 74 | — | 26 |
| 80 | 100 | 0.01 | 2 h | 76 | 24 | — |
| | | | 4 h | 68 | 32 | — |
| | | | 8 h | 64 | 36 | — |
| | | | 12 h | 42 | 53 | 5 |
| | | | 1 | 40 | 45 | 15 |
| | | | 2 | 12 | 62 | 26 |
| | | | 4 | 4 | 38 | 58 |
| | | | 8 | 4 | 3 | 93 |
| | | | 12 | 17 | — | 83 |
| | | | 16 | — | — | 100 |
| | | | 20 | — | — | 100 |
| | | | 28 | — | — | 100 |
| | | | 36 | — | — | 100 |
| 50 | 100 | 0.01 | 1 | 85 | 15 | — |
| | | | 2 | 64 | 24 | 12 |
| | | | 4 | 60 | 22 | 18 |
| | | | 8 | 32 | 36 | 32 |
| | | | 12 | 32 | 29 | 39 |
| | | | 16 | 7 | 37 | 56 |
| | | | 20 | 4 | 21 | 75 |
| | | | 28 | — | — | 100 |
| | | | 36 | — | — | 100 |

[1] P: phlogopite, V: vermiculite, P/V: interstratified mica/vermiculite.

Table 3. Chemical composition of interstratified mica/vermiculite formed after 36 days of reaction at 50°C in the 100 ml experiments.[1]

| | wt. % | Number of cations on the basis of $O_{20}(OH)_4$ | |
|---|---|---|---|
| $SiO_2$ | 44.95 | Si | 5.74 |
| $Al_2O_3$ | 17.05 | Al | 2.26 |
| $TiO_2$ | 1.14 | Ti | |
| $Fe_2O_3$ | 2.51 | Σ tet. | 8.00 |
| MgO | 25.88 | Al | 0.30 |
| $Na_2O$ | 0.93 | Ti | 0.11 |
| $K_2O$ | 7.54 | Fe | 0.54 |
| Total | 100.00 | Mg | 4.92 |
| | | Σ oct. | 5.87 |
| | | Na | 0.23 |
| | | K | 1.23 |
| | | Σ inter. | 1.46 |

[1] Ten particles were examined using AEM.

100 ml experiments. Vermiculite showed the different features unlike mica/vermiculite. In the 20 ml experiments, it appeared only in the earliest stage of reaction, however, in the 100 ml experiments, it increased in the earlier stage, but decreased later and eventually disappeared.

The representative XRD patterns after alteration runs are shown in Figure 2, in which that of phlogopite as the raw material is also illustrated. Interstratified structures can be divided into two types, as can be seen in this figure. One is R1-type interstratified mica/vermiculite, containing 60 ~ 70% mica (Figure 2a). The other is a regular 1:1 interstratified mica/vermiculite, for it shows development of both 12 Å (d(002)) and 24 Å (d(001)) peaks (Figure 2b). It was also identified in the products at 80°C in the 100 ml experiments. The CV value of the interstratified mica/vermiculite at 36 days of reaction at 50°C in the 10 ml experiments was 0.23. Table 3 shows chemical composition of interstratified mica/vermiculite formed at 36 days of reaction at 50°C in the 100 ml experiments. The interlayer of the interstratified structure is K-rich and may contain $H^+$ or $H_3O^+$ as well as a little $Na^+$.

*Elements released from phlogopite*

Figure 3 illustrates the compositional changes of solution during alteration reaction. In this figure, the concentrations of each cation released in solution from phlogopite (Tables 4 and 5) divided by each number of cation in starting material phlogopite shown in Table 2 are plotted versus time in order to represent incongruent or congruent dissolution. Hence, if each cation is released congruently in solution, lines for Si, Al, Fe, Mg and K should coincide with each other.

K was remarkably released from phlogopite until the late stage of each run, except for the period between about 20 hours and 6 days at 120°C in the 20 ml experiments and after 10 days at 80°C in the 100 ml experiments.

https://doi.org/10.1346/CCMN.1995.0430105 Published online by Cambridge University Press

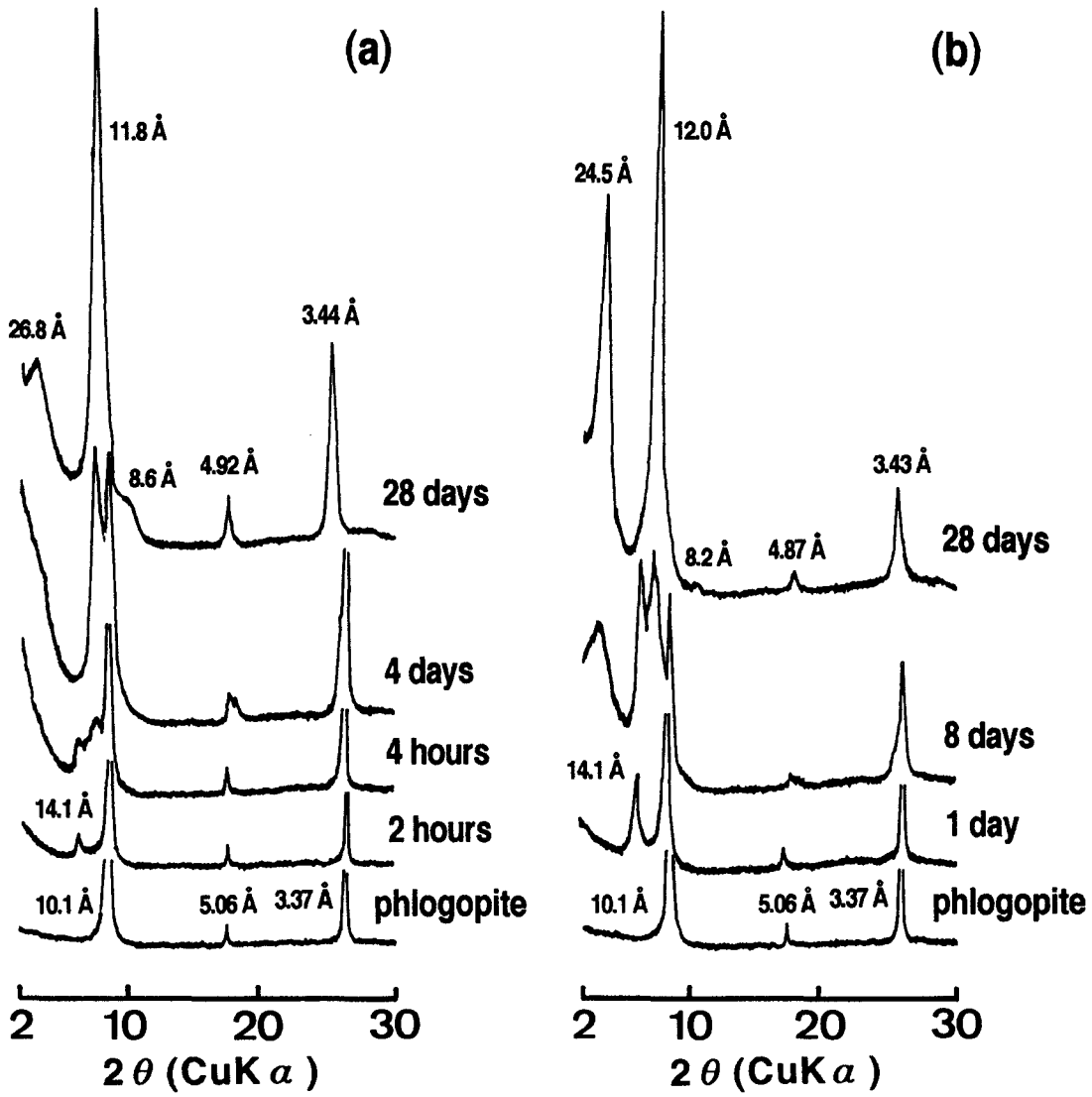



Figure 2. X-ray powder diffraction patterns of phlogopite and its alteration products after various run times (a) at 120°C in the 20 ml experiments and (b) at 50°C in the 100 ml experiments.

At 80° and 50°C in the 20 ml experiments, all of the elements except for K are likely congruent. At 120°C, Si and Mg were removed at approximately the same rate, but Fe was released more easily than K from about 20 hours to 6 days and decreased after 6 days, and Al was released most slowly compared with all other elements in phlogopite. On the other hand, in the 100 ml experiments, it can be seen from the slope of each line in Figure 3 that the dissolution priority is in the order; K > Fe > Mg, Al > Si in the initial stage. The pH value increased rapidly in the 20 ml experiments, especially at 120°C. It, however, changed barely in the 100 ml experiments.

Figure 4 shows the time-changes of ratio of instantaneous release rates of K to Si ($r_{K/1.80}/r_{Si/5.74}$) and those of Mg to Si ($r_{Mg/5.58}/r_{Si/5.74}$) under the dissolution of phlogopite. This rate shows the change of concentration of element in solution per unit time (hour) before and after a time in Figure 3. The release rate of K or Mg becomes congruent relative to that of Si in the time interval when the ratio is 1.

At 120° and 80°C in the 20 ml experiments, the period that $r_{K/1.80}/r_{Si/5.74}$ ratio is greater than 1, which means that the release rate of K is faster than that of Si, appears two times during the 28 days run. At 120°C, the first is in the early stage up to about 8 hours of reaction and the second is in the later stage between about 1 and 20 days of reaction. At 80°C, the first is up to 6 days and the second is after 16 days of reactions. On the other hand, in the 100 ml experiments, $r_{K/1.80}/$

https://doi.org/10.1346/CCMN.1995.0430105 Published online by Cambridge University Press

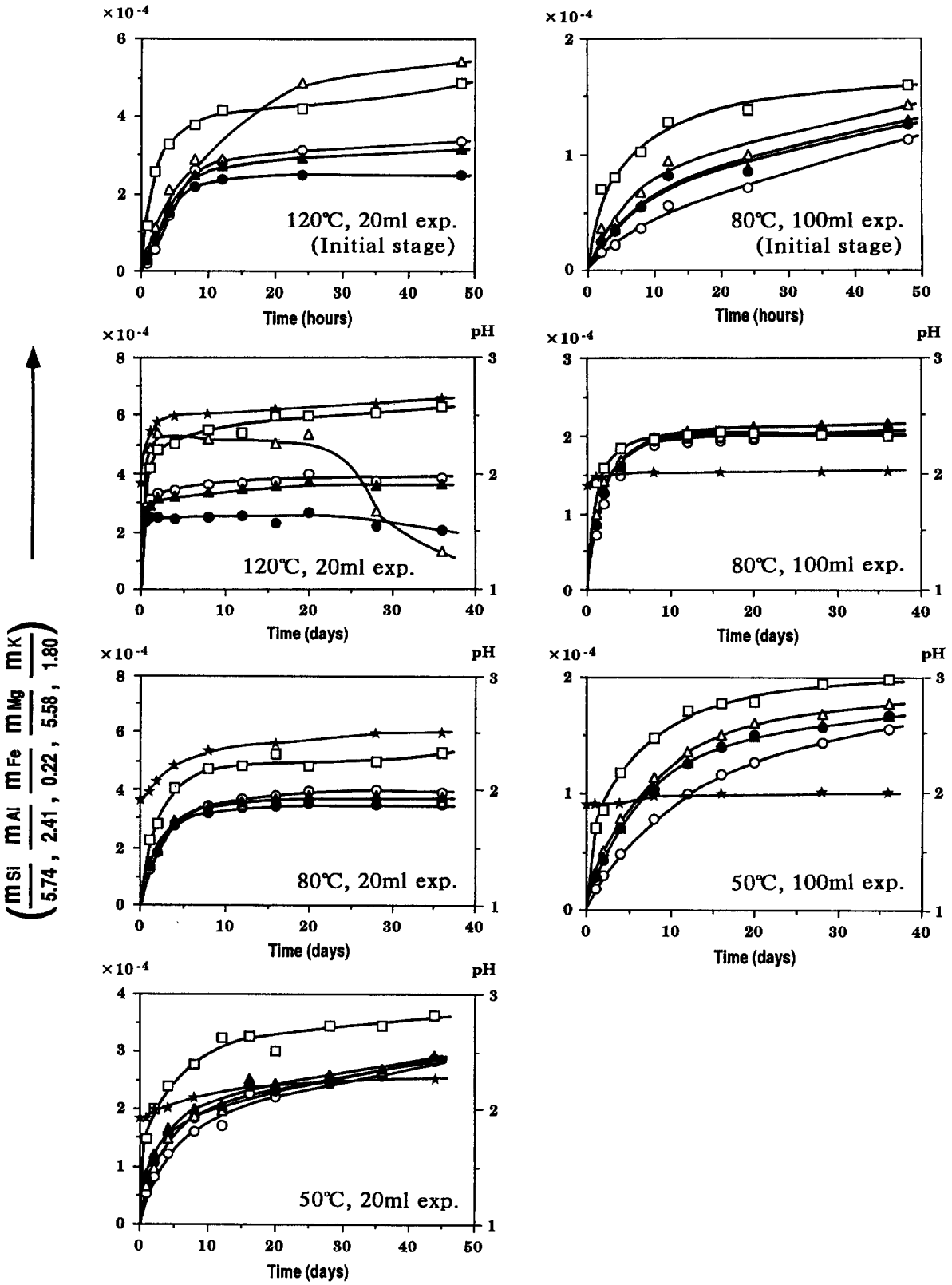



Figure 3. Plots for deviation from congruent dissolution of phlogopite in the 20 ml and 100 ml experiments. The concentrations of Si, Al, Fe, Mg and K released in solution were divided by the number of each cation of phlogopite shown in Table 1. ○: Si, ●: Al, △: Fe, ▲: Mg, □: K, ★: pH.

https://doi.org/10.1346/CCMN.1995.0430105 Published online by Cambridge University Press

Table 4. Chemical compositions and pH values of solutions after each run time for 20 ml experiments.

| T (°C) | Duration (days) | Concentration ($10^{-4}$ mol/liter) | | | | | Conc. (mol/liter)/number of cation[1] ($10^{-5}$) | | | | | |
|---|---|---|---|---|---|---|---|---|---|---|---|---|
| | | Si | Al | Fe | Mg | K | Si/5.74 | Al/2.41 | Fe/0.22 | Mg/5.58 | K/1.80 | pH[2] |
| 120 | 1 hour | 1.2 | 0.6 | 0.1 | 2.1 | 2.1 | 2.1 | 2.7 | 5.0 | 3.8 | 11.7 | 2.00 |
| | 2 h | 3.1 | 1.9 | 0.2 | 5.1 | 4.6 | 5.5 | 8.0 | 11.3 | 9.1 | 25.6 | 2.03 |
| | 4 h | 8.3 | 3.6 | 0.5 | 9.6 | 5.9 | 14.4 | 15.1 | 20.9 | 17.2 | 32.6 | 2.11 |
| | 8 h | 14.9 | 5.3 | 0.6 | 14.0 | 6.8 | 25.9 | 22.0 | 28.8 | 25.1 | 37.8 | 2.22 |
| | 12 h | 16.2 | 5.7 | 0.6 | 15.2 | 7.5 | 28.2 | 23.6 | 28.9 | 27.2 | 41.7 | 2.24 |
| | 1 | 17.8 | 6.0 | 1.1 | 16.3 | 7.6 | 31.0 | 25.0 | 48.6 | 29.2 | 42.1 | 2.29 |
| | 2 | 19.1 | 6.0 | 1.2 | 17.7 | 8.7 | 33.3 | 24.9 | 53.9 | 31.7 | 48.6 | 2.34 |
| | 4 | 19.7 | 5.9 | 1.1 | 18.1 | 9.1 | 34.3 | 24.4 | 51.1 | 32.4 | 50.4 | 2.36 |
| | 8 | 20.8 | 6.0 | 1.1 | 18.9 | 9.9 | 36.3 | 25.0 | 51.7 | 33.9 | 54.9 | 2.43 |
| | 12 | 21.1 | 6.1 | 1.2 | 19.4 | 9.7 | 36.8 | 25.3 | 53.8 | 34.8 | 54.1 | 2.53 |
| | 16 | 21.4 | 5.5 | 1.1 | 19.9 | 10.8 | 37.3 | 22.9 | 50.5 | 35.7 | 59.9 | 2.60 |
| | 20 | 22.9 | 6.3 | 1.2 | 20.8 | 10.7 | 39.8 | 26.3 | 53.3 | 37.2 | 59.5 | 2.62 |
| | 28 | 21.4 | 5.2 | 0.6 | 19.9 | 10.9 | 37.3 | 21.7 | 27.3 | 35.6 | 60.7 | 2.60 |
| | 36 | 22.0 | 4.9 | 0.3 | 20.3 | 11.3 | 38.4 | 20.5 | 12.8 | 36.4 | 63.0 | 2.62 |
| 80 | 1 | 7.3 | 3.2 | 0.3 | 8.4 | 4.0 | 12.7 | 13.3 | 14.5 | 15.1 | 22.2 | 2.03 |
| | 2 | 10.3 | 4.3 | 0.4 | 10.8 | 5.1 | 17.9 | 18.0 | 18.6 | 19.3 | 28.2 | 2.11 |
| | 4 | 16.2 | 6.6 | 0.6 | 16.2 | 7.3 | 28.3 | 27.3 | 28.9 | 29.0 | 40.5 | 2.31 |
| | 8 | 19.7 | 7.6 | 0.7 | 18.7 | 8.5 | 34.4 | 31.4 | 33.2 | 33.6 | 47.3 | 2.40 |
| | 12 | 21.2 | 8.1 | 0.8 | 20.0 | 8.7 | 36.9 | 33.7 | 35.0 | 35.9 | 48.5 | 2.50 |
| | 16 | 21.8 | 8.3 | 0.8 | 20.5 | 9.5 | 37.9 | 34.5 | 36.2 | 36.8 | 52.6 | 2.54 |
| | 20 | 22.6 | 8.5 | 0.8 | 21.2 | 8.7 | 39.4 | 35.3 | 37.9 | 38.1 | 48.4 | 2.58 |
| | 28 | 22.9 | 8.4 | 0.8 | 21.3 | 9.0 | 39.9 | 34.8 | 37.7 | 38.1 | 49.8 | 2.62 |
| | 36 | 22.4 | 8.3 | 0.8 | 20.7 | 9.6 | 39.0 | 34.6 | 36.1 | 37.2 | 53.2 | 2.67 |
| 50 | 1 | 3.0 | 1.6 | 0.1 | 4.7 | 2.7 | 5.2 | 6.8 | 6.4 | 8.5 | 14.9 | 1.91 |
| | 2 | 4.6 | 2.5 | 0.2 | 6.8 | 3.6 | 8.0 | 10.5 | 9.6 | 12.1 | 19.9 | 1.96 |
| | 4 | 6.9 | 3.8 | 0.3 | 9.3 | 4.3 | 12.1 | 15.6 | 14.9 | 16.7 | 24.0 | 2.04 |
| | 8 | 9.3 | 4.5 | 0.4 | 11.2 | 5.0 | 16.2 | 18.6 | 18.7 | 20.0 | 27.7 | 2.10 |
| | 12 | 9.9 | 4.8 | 0.4 | 11.5 | 5.8 | 17.2 | 19.9 | 19.8 | 20.6 | 32.5 | 2.10 |
| | 16 | 12.9 | 5.8 | 0.5 | 14.0 | 5.9 | 22.5 | 24.0 | 24.6 | 25.1 | 32.8 | 2.19 |
| | 20 | 12.6 | 5.6 | 0.5 | 13.6 | 5.4 | 22.0 | 23.2 | 24.1 | 24.3 | 30.0 | 2.16 |
| | 28 | 14.0 | 6.0 | 0.6 | 14.4 | 6.2 | 24.4 | 24.9 | 25.8 | 25.8 | 34.6 | 2.19 |
| | 36 | 15.1 | 6.2 | 0.6 | 15.1 | 6.2 | 26.2 | 25.8 | 26.6 | 27.1 | 34.6 | 2.28 |

[1] Concentration (mol/liter) of Si, Al, Fe, Mg, and K in solution were divided by the number of each cation of phlogopite shown in Table 1.
[2] Starting pH = 1.90.

$r_{Si/5.74}$ ratio is greater than 1 up to about 1 and 8 days of reaction at 80° and 50°C, respectively, since then, this ratio becomes much less than 1. This indicates that the release of K is outwardly slower than that of Si after 1 and 8 days of reaction at 80° and 50°C, respectively. The second selective release of K relative to Si as observed in the 20 ml experiments is not found in the 100 ml experiments.

*Transmission electron microscopy*

Figure 5 shows a lattice fringe image of starting material phlogopite. This phlogopite is composed of packets of several layers. The thickness of individual packet varies from about 50 Å to 500 Å within the observed samples. The lattice fringe image within the packet is homogeneous in contrast and parallel to each other.

Figure 6 illustrates a lattice fringe image of an alteration product in the initial stage (1 day) at 80°C in the 20 ml experiments. Vermiculite occurs sporadically throughout the phlogopite, intersects the particle, and separates the still-contracted packets of several layers. The basal spacings of vermiculite saturated with hydrated metal cations are generally unstable under the P, T-conditions in the electron beam (Marcks *et al* 1989). Therefore, basal spacings of vermiculite have shown 14 Å (e.g., Banfield and Eggleton 1988) and/or 10 Å (e.g., Vali and Köster 1986) corresponding to "collapsed" vermiculite. The still-contracted packets are composed of between two and eleven mica layers. Vermiculite-vermiculite sequences (VVVV . . .) are not observed and the still-contracted packets are bounded by single vermiculite layers. These are also shown in the early stage at 120°C in the 20 ml experiments.

A periodic interstratification of the still-contracted packet composed of between two and seven 10 Å layers and mica-vermiculite sequence (MVMV . . .) composed of between one and four two-layers 20 Å units was found in the late stage of reaction at 120°C in the 20 ml experiments (Figure 7). Domains of the still-contracted packets apparently decreased with the progress of reaction.

In the early stage of the 100 ml experiments, it was

https://doi.org/10.1346/CCMN.1995.0430105 Published online by Cambridge University Press

Table 5. Chemical compositions and pH values of solutions after each run time for 100 ml experiments.

| T (°C) | Duration (days) | Concentration ($10^{-4}$ mol/liter) | | | | | Conc. (mol/liter)/number of cation ($10^{-5}$) | | | | | pH |
|---|---|---|---|---|---|---|---|---|---|---|---|---|
| | | Si | Al | Fe | Mg | K | Si/5.74 | Al/2.41 | Fe/0.22 | Mg/5.58 | K/1.80 | |
| 80 | 2 hour | 0.9 | 0.6 | 0.1 | 1.5 | 1.3 | 1.5 | 2.4 | 3.6 | 2.7 | 7.0 | 1.91 |
| | 4 h | 1.2 | 0.8 | 0.1 | 2.0 | 1.4 | 2.2 | 3.4 | 4.3 | 3.6 | 8.0 | 1.91 |
| | 8 h | 2.1 | 1.3 | 0.1 | 3.1 | 1.8 | 3.7 | 5.4 | 6.8 | 5.6 | 10.2 | 1.93 |
| | 12 h | 3.2 | 2.0 | 0.2 | 4.7 | 2.3 | 5.6 | 8.2 | 9.5 | 8.5 | 12.8 | 1.97 |
| | 1 | 4.1 | 2.1 | 0.2 | 4.9 | 2.5 | 7.1 | 8.6 | 10.0 | 8.8 | 13.9 | 1.97 |
| | 2 | 6.5 | 3.0 | 0.3 | 7.3 | 2.9 | 11.3 | 12.6 | 14.2 | 13.0 | 16.0 | 2.00 |
| | 4 | 8.6 | 3.9 | 0.4 | 9.1 | 3.3 | 15.0 | 16.1 | 17.0 | 16.2 | 18.6 | 2.04 |
| | 8 | 10.8 | 4.7 | 0.4 | 11.0 | 3.5 | 18.8 | 19.5 | 19.7 | 19.8 | 19.7 | 2.10 |
| | 12 | 11.1 | 4.8 | 0.4 | 11.5 | 3.6 | 19.3 | 19.9 | 19.9 | 20.7 | 20.2 | 2.07 |
| | 16 | 11.1 | 4.8 | 0.4 | 11.5 | 3.7 | 19.4 | 19.9 | 20.1 | 20.6 | 20.6 | 2.11 |
| | 20 | 11.2 | 4.9 | 0.4 | 11.8 | 3.7 | 19.6 | 20.4 | 19.9 | 21.2 | 20.5 | 2.10 |
| | 28 | 11.6 | 5.0 | 0.5 | 12.0 | 3.6 | 20.2 | 20.8 | 20.5 | 21.5 | 20.0 | 2.11 |
| | 36 | 11.5 | 5.0 | 0.4 | 12.1 | 3.6 | 20.0 | 20.7 | 20.3 | 21.7 | 20.0 | 2.12 |
| 50 | 1 | 1.1 | 0.7 | 0.1 | 1.6 | 1.3 | 1.8 | 2.8 | 3.3 | 2.9 | 7.0 | 1.90 |
| | 2 | 1.7 | 1.0 | 0.1 | 2.5 | 1.5 | 2.9 | 4.3 | 5.1 | 4.5 | 8.6 | 1.90 |
| | 4 | 2.8 | 1.7 | 0.2 | 3.9 | 2.1 | 4.8 | 7.0 | 7.8 | 7.0 | 11.8 | 1.92 |
| | 8 | 4.5 | 2.5 | 0.3 | 5.8 | 2.7 | 7.8 | 10.4 | 11.4 | 10.4 | 14.8 | 1.96 |
| | 12 | 5.7 | 3.0 | 0.3 | 7.1 | 3.1 | 10.0 | 12.6 | 13.6 | 12.7 | 17.1 | 1.98 |
| | 16 | 6.7 | 3.4 | 0.3 | 7.9 | 3.2 | 11.7 | 14.1 | 15.0 | 14.1 | 17.8 | 2.02 |
| | 20 | 7.3 | 3.6 | 0.4 | 8.4 | 3.2 | 12.7 | 15.1 | 16.1 | 15.0 | 17.9 | 2.01 |
| | 28 | 8.3 | 3.8 | 0.4 | 8.9 | 3.5 | 14.4 | 15.8 | 16.9 | 15.9 | 19.5 | 2.03 |
| | 36 | 9.0 | 4.0 | 0.4 | 9.3 | 3.6 | 15.6 | 16.7 | 17.8 | 16.7 | 19.9 | 2.04 |

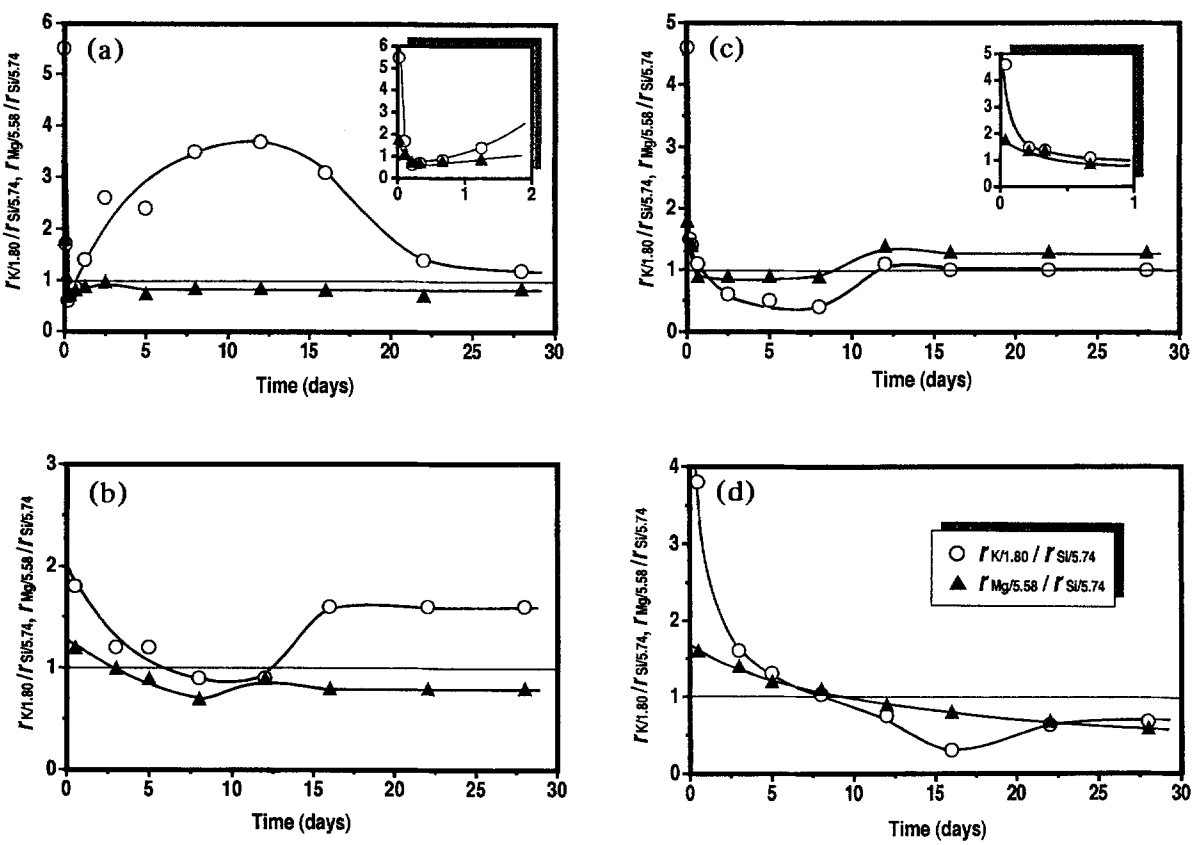



Figure 4. Plots of ratio of instantaneous release rates of K to Si ($r_{K/1.80}/r_{Si/5.74}$) and Mg to Si ($r_{Mg/5.58}/r_{Si/5.74}$) vs. time for dissolution of phlogopite. The release rate of K or Mg becomes congruent relative to Si when the ratio is 1. (a) at 120°C and (b) 80°C in the 20 ml experiments, (c) at 80°C and (d) 50°C in the 100 ml experiments.

https://doi.org/10.1346/CCMN.1995.0430105 Published online by Cambridge University Press

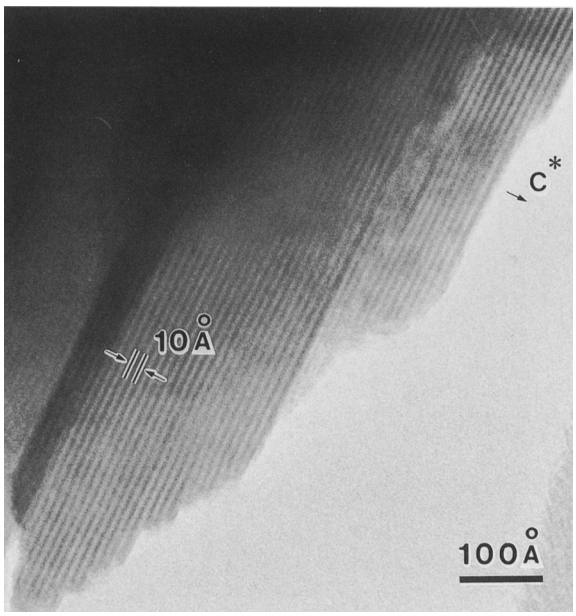



Figure 5. Lattice fringe image of untreated phlogopite.

not found that single vermiculite layer occurred sporadically throughout the particle as shown in the 20 ml experiments. Random arrangements of 10 Å and 20 ~ 23 Å basal spacings were often observed until the middle stage of reaction in the 100 ml experiments. Figure 8 shows lattice fringe image of interstratified mica/vermiculite illustrating the formation of mica-vermiculite pairs in the late stage at 50°C in the 100 ml experiments. Two-layer 20 Å periodicity generally develops over the longer range than in the 20 ml experiments. When compared to the structure of starting material phlogopite shown in Figure 5, the symmetry of the layer arrangement is reduced by the bending of layers, giving rise to an undulated appearance of the lattice.

## DISCUSSION

### *Incongruent dissolution of phlogopite*

Figure 3 indicates that the preferential release of K from phlogopite occurs in almost all stages of alteration. Nagasawa *et al* (1974) carried out alteration experiments of biotite with $AlCl_3$ solution and explained that K in mica was released more rapidly than other elements because the replacement reaction of the interlayer K by Al as well as bulk dissolution of biotite was occurring during the alteration process. In the present experiments, the preferential release of K from phlogopite is likely accelerated by exchange reaction with $H^+$ and $Na^+$ present in solution. Consequently, a K-depleted layer is formed and the secondary phases vermiculite and/or interstratified mica/vermiculite are found.

The behavior of Fe, Mg, and Al in the 20 ml experiments is somewhat different from that in the 100 ml experiments. In the latter except for the period after 10 days at 80°C, the priority in dissolution is in the order; K > Fe > Mg, Al > Si. Schott *et al* (1981) have explained that the incongruent dissolution found in the dissolution experiments of enstatite, diopside, and tremolite especially in the initial stage is likely due to binding energy difference. It has also been described that clay leaching is controlled by mineral structure (Casey and Bunker 1990). Crystallographically, clays consist of sheets of $Q^3$ silicon tetrahedra separated by layers of octahedral magnesium- or aluminum-hydroxide. Both the magnesium-hydroxide and aluminum-hydroxide sheets are unstable in an acid solution relative to the silicate structure. Thus clay leaching generally proceeds inward along the octahedral layer from the edges of the phyllosilicate. The crystal structure of mica consists of negatively charged 2:1 layer, which contains two tetrahedral sheets and one octahedral sheet. They are linked together by large, positively charged, interlayer cation and the electric charge is compensated. The bonds between the interlayer species and the oxygenated surfaces of the 2:1 layers are weaker than the T-O-T bonds. Thus, phlogopite leaching may proceed inward along the interlayer space and octahedral sheet from the edges of the crystal.

On the other hand, at 80° and 50°C in the 20 ml experiments, the release of Mg, Fe, and Al from phlogopite is nearly congruent relative to Si, but at 120°C, the contents of Fe and Al in solution decrease after about 6 days and 12 hours of reaction, respectively. The precipitation of secondary phases occurs particularly in case of Al and Fe silicates under acid condition in batch system, in which the composition of the reacting solution changes and pH value increases continuously with time (Schott and Petit 1987, Tsuzuki *et al* 1985). In the present experiments, the composition of the reacting solution and pH value change more rapidly in the 20 ml experiments, particularly at 120°C, than in the 100 ml experiments, because the volume of solution in the former (20 ml) is smaller than that in the latter (100 ml). The decrease of Al and Fe in solution at 120°C is probably due to the precipitation of secondary phases such as aluminum and iron oxides and/or hydroxides.

### *Transformation process of phlogopite to interstratified mica/vermiculite*

Two processes are confirmed on the formation of interstratified structure from the results described above:

(1) Interstratified structure is formed directly from phlogopite (in the 20 ml experiments).
(2) Interstratified structure is formed from vermiculite which was produced earlier from phlogopite by the

https://doi.org/10.1346/CCMN.1995.0430105 Published online by Cambridge University Press




Figure 6. Lattice fringe image illustrating sporadic distribution of single vermiculite layer (↓) after 1 day of reaction at 80°C in the 20 ml experiments.

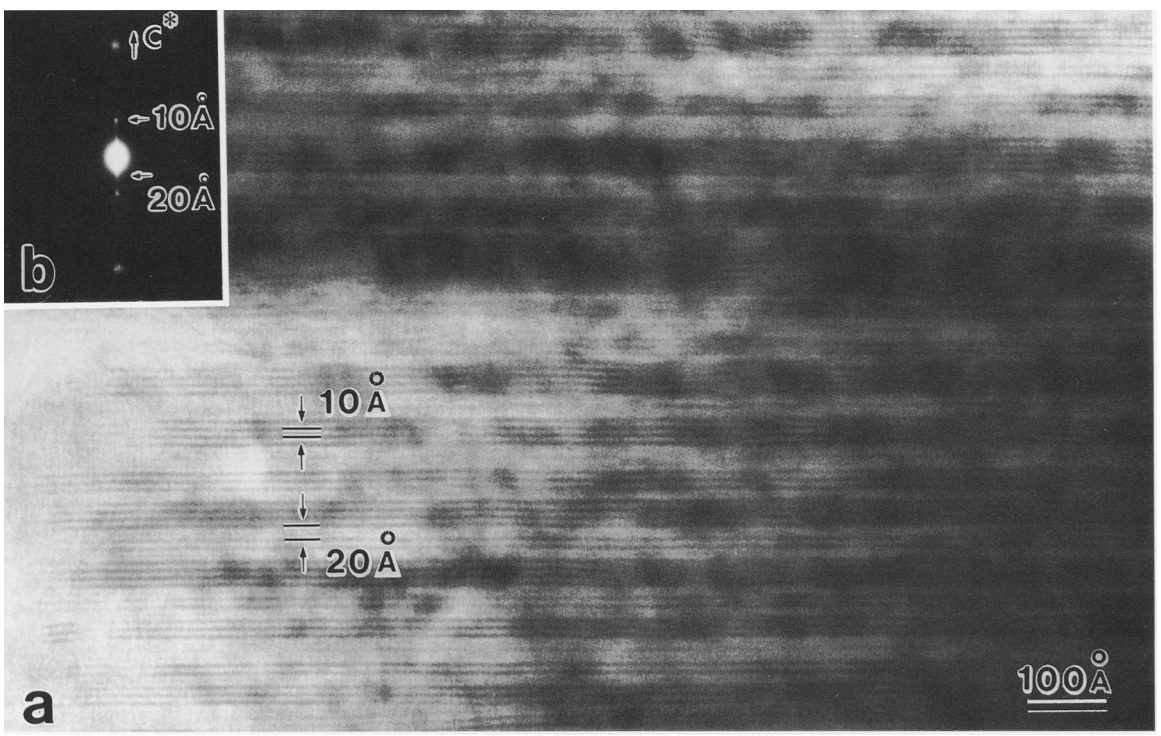



Figure 7. (a) Lattice fringe image illustrating a periodic interstratification of the still-contracted packets composed of between two and seven 10 Å layers and the mica-vermiculite sequences composed of between one and three 20 Å units in the late stage (28 days) at 120°C in the 20 ml experiments. (b) Selected area electron diffraction pattern of the region shown in (a).

https://doi.org/10.1346/CCMN.1995.0430105 Published online by Cambridge University Press

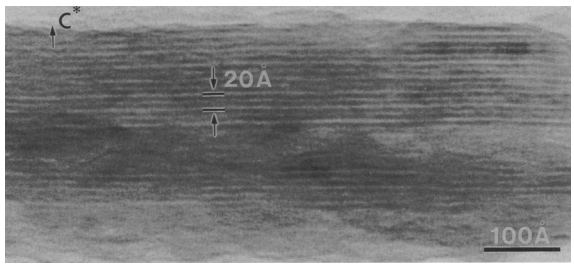



Figure 8. Lattice fringe image illustrating the formation of mica-vermiculite pairs in the late stage (36 days) at 50°C in the 100 ml experiments.

regaining of K from the ambient solution (in the 100 ml experiments).

At 120°C in the 20 ml experiments, bulk dissolution of starting material progresses rapidly up to about two days of reaction and then becomes apparently slow (Figure 9). The formation of vermiculite in the earliest stage corresponds to the first preferential release of K relative to Si as shown in Figure 4. This vermiculite disappears immediately. The formation of interstratified mica/vermiculite with decrease of phlogopite corresponds to the first and second selective release of K relative to Si. It can be seen from Table 2 and Figure 4 that a variation similar to that at 120°C in the 20 ml experiments occurred at 80°C, too.

On the other hand, in the 100 ml experiments, released K is concentrated to a certain extent into the reacting solution during reaction, since vermiculite is formed much greater than in the 20 ml experiments and bulk dissolution progresses swiftly (Figure 9). After that, the increase of interstratified mica/vermiculite was observed after 8 days of reaction, although the release of K is outwardly inhibited relative to Si. Inoue *et al* (1981) demonstrated that the regaining of K by vermiculite occurs at a fairly low concentration of K in the solution, such as that lower than 10 ppm. It is also expected from Table 3 that mica-like interlayer cation in the interstratified structure is K-rich rather than Na-rich. Therefore, the outwardly inhibitive release of K relative to Si in the middle and late stages of the 100 ml experiments is due to the regaining of K by vermiculite from the ambient solution.

As regards the direct transformation of phlogopite to interstratified mica/vermiculite, it is clear from TEM observation of samples in the 20 ml experiments that mica-vermiculite sequences apparently developed sequentially outward from an initial vermiculite layer which occurred sporadically throughout the phlogopite grain (Figures 6 and 7). Initially, single vermiculite layer occurs sporadically throughout the phlogopite, then, a periodic interstratification of the still-contracted packet and the short-ranged mica-vermiculite sequence develops with the progress of reaction. A number of initial single vermiculite layers disappear and

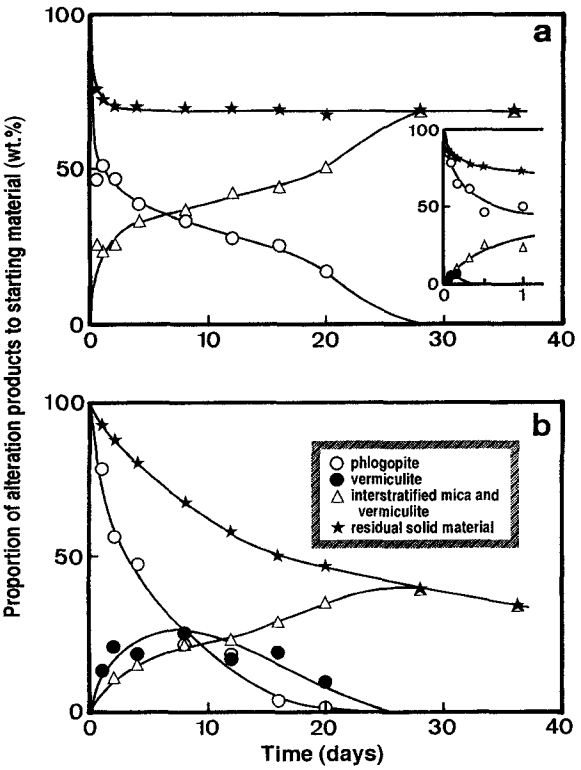



Figure 9. Plots of proportion of alteration products and residual solid material to starting material (20 mg) vs. time. (a) At 120°C in the 20 ml experiments. (b) At 50°C in the 100 ml experiments.

domains of the still-contracted packets apparently decrease with the progress of reaction.

On the other hand, in the early stage of the 100 ml experiments, the sporadic distribution of single vermiculite layer and mica-vermiculite sequences shown in the 20 ml experiments were not observed. In the middle and late stage of the 100 ml experiments, two-layer 20 Å periodicity corresponding to mica-vermiculite sequence developed instead of vermiculite-vermiculite sequences (Figure 8). This supports that interstratified mica/vermiculite (R1) is formed from vermiculite which was formed earlier from phlogopite by the regaining of K from the ambient solution.

### *The effect of the release rate of K on the development of mica-vermiculite and vermiculite-vermiculite sequences*

Rausell-Colom *et al.* (1965) and Hoda and Hood (1972) have stated that interstratification would be expected in dilute salt solution and the slow replacement of K, as natural weathering. From recent TEM study, it has been illustrated that in natural weathering single vermiculite layer occurred sporadically throughout the mica grain, or mica-vermiculite pairs developed (Banfield and Eggleton 1988). In contrast, Reichenbach *et*

https://doi.org/10.1346/CCMN.1995.0430105 Published online by Cambridge University Press

*al* (1988) showed that vermiculite-vermiculite sequences developed from a mica sample which altered in batch-flow system experiments. The mica was gradually transformed to vermiculite by repeated treatment with 0.1 N $BaCl_2$ solution.

From the results of the present experiments, it cannot be explained whether ionic strength of solution influences the transformation of mica or not. However, it seems to depend on the release rate of K from phlogopite whether it transforms to vermiculite or interstratified structure. The release of K during the formation of vermiculite-vermiculite sequences is faster than that during the period in which mica-vermiculite sequences are mainly formed. The K exchange mechanism is a diffusion-controlled process (Mortland 1958, Reed and Scott 1962, Leonard and Weed 1970). In acid dissolution reactions involving diffusion, the data have been applied to the parabolic rate low, $\alpha = kt^{1/2}$ where $\alpha$ is the fraction of the initial amount of cations dissolved at time t and k is the rate constant (Ross 1967). From Figure 10 obtained from above equation, the rate constants of K-release between 0 and 12 hours of reaction at 120°C in the 20 ml experiments, between 0 and 12 hours at 80°C in the 100 ml experiments, and between 0 and 8 days at 50°C in the 100 ml experiments which phlogopite transforms mainly to vermiculite were 0.06, 0.09 and 0.03 $hour^{-1/2}$, respectively. In contrast, the rate constants of K-release between 12 hours and 28 days of reaction at 120°C in the 20 ml experiments and between 4 and 36 days at 80°C in the 20 ml experiments which phlogopite transformed directly to interstratified structure were 0.005 and 0.002 $hour^{-1/2}$, respectively. No vermiculite-vermiculite sequences have been found from samples of the later by TEM observation.

However, it is not clear why ordered interstratified-layering should occur. Norrish (1973) proposed that the formation of regularity in mica-vermiculite layer sequences is related to the change in hydroxyl orientation in the layers adjacent to one from which K had been removed, causing firmer bonding of the K in these layers. If the development of regular interstratification results from the above mechanism, there may be a certain range of release rate of K within which the mechanism comes into play.

## CONCLUSIONS

The dissolution of phlogopite in acid solution occurs incongruently and the preferential release of K occurs in all stages of the alteration. The priority in dissolution in the 100 ml experiments is in the order; K > Fe > Mg, Al > Si. This supports that phlogopite leaching is controlled by the mineral structure as the leaching proceeds along the interlayer space (and the octahedral sheet). In the 20 ml experiment, the amounts of Al and Fe released from phlogopite decrease with the progress of reaction at higher temperature. The composition of

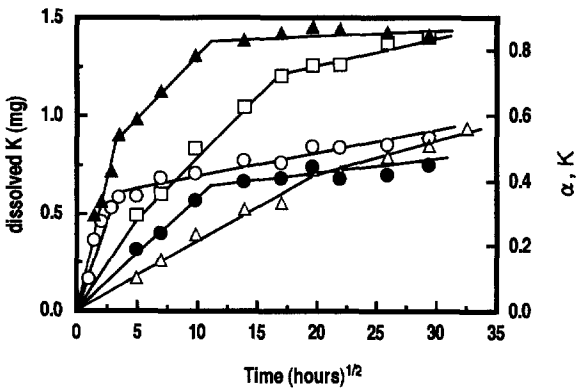



Figure 10. Plots of the amount (mg) of K dissolved from phlogopite or fraction dissolved ($\alpha$) of K from phlogopite vs. $time^{1/2}$ ○: at 120°C, ●: at 80°C, and △: at 50°C in the 20 ml experiments, and ▲: at 80°C and □: at 50°C in the 100 ml experiments.

reacting solution and pH value change more rapidly when the volume of solution is small, and particularly under higher temperature. In this case, the decrease of the amounts of Al and Fe in solution is due to the precipitation of secondary phases such as aluminum and iron oxides and/or hydroxides.

Interstratified structure is formed (1) directly from phlogopite or (2) from vermiculite which was produced earlier from phlogopite by regaining of K from the ambient solution. It seems to depend on the release rate of K from phlogopite whether vermiculite-vermiculite sequences develop or mica-vermiculite sequences do. The former develops only when the release rate of K is sufficiently faster than that of K during the period in which the latter is mainly formed.

## ACKNOWLEDGMENTS

We are grateful to Dr. Yoshihiro Nakamuta of Kyushu University for permission to use his profile fitting program and valuable suggestions in the course of this work, Dr. Seiichiro Uehara of Kyushu University for assistance with the operation of TEM and many discussions, Dr. Masanori Matsui of Kyushu University for helpful suggestions. We also thank the staff of the Research Laboratory of High Voltage Electron Microscope, Kyushu University for access to and assistance with the operation of TEM, Mr. Kazuhiko Shimada for electron microprobe analyses, Dr. Tadao Nishiyama of Kyushu University and Dr. Masaharu Ozaki of Kumamoto University for assistance with the operation of ICP-AES.

## REFERENCES

Banfield, J. F., and R. A. Eggleton 1988. Transmission electron microscope study of biotite weathering. *Clays & Clay Miner.* **36**: 47–60.

Barshad, I. 1948. Vermiculite and its relation to biotite as revealed by base exchange reactions, X-ray analyses, dif-

https://doi.org/10.1346/CCMN.1995.0430105 Published online by Cambridge University Press

ferential thermal curves and water content. *Amer. Miner.* **33**: 665–678.

Boettcher, A. L. 1966. Vermiculite, hydrobiotite, and biotite in the Rainy Creek igneous complex near Libby, Montana. *Clay Miner.* **6**: 283–296.

Brindley, G. W., P. E. Zalba, and C. M. Bethke. 1983. Hydrobiotite, a regular 1:1 interstratification of biotite and vermiculite layers. *Amer. Miner.* **68**: 420–425.

Casey, W. H., and B. Bunker. 1990. Leaching of mineral and glass surfaces during dissolution. In *Mineral-Water Interface Geochemistry, Reviews in Mineralogy, Vol. 23.* M. F. Hochella Jr. and A. F. White, eds. Mineralogical Society of America, 397–426.

Hoda, S. N., and W. C. Hood. 1972. Laboratory alteration of trioctahedral micas. *Clays & Clay Miner.* **20**: 343–358.

Inoue, A., I. Shimizu, and H. Minato. 1981. Mass transfer during alteration of phlogopite in calcium-bearing acid aqueous solution. *Clay Sci.* **5**: 283–297.

Leonard, R. A., and S. B. Weed. 1970. Mica weathering rates as related to mica type and composition. *Clays & Clay Miner.* **18**: 187–195.

Marcks, C. H., H. Wachsmuth, and H. G. V. Reichenbach. 1989. Preparation of vermiculites for HRTEM. *Clay Miner.* **24**: 23–32.

Mortland, M. M. 1958. Kinetics of potassium release from biotite. *Soil Sci. Soc. Amer. Proc.* **22**: 503–508.

Nagasawa, K., G. Brown, and A. C. D. Newman. 1974. Artificial alteration of biotite into a 14 Å layer silicate with hydroxy-aluminum interlayers. *Clays & Clay Miner.* **22**: 241–252.

Nakamuta, Y., N. Shimada, and Y. Aoki. 1991. Analysis of X-ray powder diffraction peak profiles of optically anomalous cassiterite by profile fitting method. *Advances in X-ray Chem. Anal. Japan* **22**: 243–252 (in Japanese).

Norrish, K. 1973. Factors in the weathering of mica to vermiculite. In *Proc. Int. Clay Conf., Madrid, 1972.* J. M. Serratosa, ed. Madrid: Div. Ciencias C. S. I. C., 417–432.

Rausell-Colom, J., T. R. Sweatman, C. B. Wells, and K. Norrish. 1965. Studies in the artificial weathering of micas. *Experimental Pedology, Proc. 11th. School Agric.,* Nottingham, 40–72.

Reed, M. G., and A. D. Scott. 1962. Kinetics of potassium release from biotite and muscovite in sodium tetraphenylboron solutions. *Soil Sci. Soc. Amer. Proc.* **26**: 437–440.

Reichenbach, H. G. V., H. Wachsmuth, and C. Marcks. 1988. Observations at the mica-vermiculite interface with HRTEM. *Colloid Polym. Sci.* **266**: 652–656.

Rhcades, J. D., and N. T. Coleman. 1967. Interstratification in vermiculite and biotite produced by potassium sorption. I. Evaluation by simple X-ray diffraction pattern inspection. *Soil Sci. Soc. Amer. Proc.* **31**: 366–372.

Ross, G. J. 1967. Kinetics of dissolution of an orthochlorite mineral. *Canad. J. Chem.* **45**: 3031–3034.

Sawhney, B. L. 1969. Regularity of interstratification as affected by charge density in layer silicates. *Soil Sci. Soc. Amer. Proc.* **33**: 42–46.

Schnitzer, M., and H. Kodama. 1976. The dissolution of micas by fulvic acid. *Geoderma* **15**: 381–391.

Schott, J., R. A. Berner, and E. L. Sjöberg. 1981. Mechanism of pyroxene and amphibole weathering. I. Experimental studies of iron-free minerals. *Geochim. Cosmochim. Acta* **45**: 2123–2135.

Schott, J., and J. C. Petit. 1987. New evidence for the mechanisms of dissolution of silicate minerals. In *Aquatic Surface Chemistry.* W. Stumm, ed. New York: Wiley-Interscience, 293–315.

Tsuzuki, Y. 1985. Thermodynamics and kinetics of weathering and hydrothermal alteration. *Jour. Geol. Soc. Japan* **91**: 699–718 (in Japanese).

Tsuzuki, Y., S. Kadota, and I. Takashima. 1985. Dissolution process of albite and albite glass in acid solutions at 47°C. *Chem. Geol.* **49**: 127–140.

Vali, H., and H. M. Köster. 1986. Expanding behaviour, structural disorder, regular and random irregular interstratification of 2:1 layer-silicates studied by high-resolution images of transmission electron microscopy. *Clay Miner.* **21**: 827–859.

Walker, G. F. 1949. The decomposition of biotite in the soil. *Mineral. Mag.* **28**: 693–703.

Wilson, M. J. 1966. The weathering of biotite in some Aberdeenshire soils. *Mineral. Mag.* **35**: 1080–1093.

Wilson, M. J. 1970. A study of weathering in a soil derived from a biotite-hornblende rock. I. Weathering of biotite. *Clay Miner.* **8**, 291–303.

*(Received 21 December 1993; accepted 6 July 1994; Ms. 2447)*

https://doi.org/10.1346/CCMN.1995.0430105 Published online by Cambridge University Press